EPJ Web of Conferences **368**, 00007 (2026) https://doi.org/10.1051/epjconf/202636800007
HIAS 2025

Modelling Energy Dissipation in a Time-Dependent Coupled Channels Model for Fusion

M. M. Webber[1,*], E. C. Simpson[1], and J. Buete[1]

[1]Department of Nuclear Physics and Accelerator Applications, Research School of Physics, The Australian National University, Canberra, ACT 2601, Australia

Abstract. To describe fusion, coupled channels models typically implement an absorbing potential or incoming wave boundary condition to capture incoming flux that penetrates the fusion barrier. These flux-trapping conditions obscure the dissipative processes that lead to fusion, preventing any understanding of how the apparently irreversible thermalisation of the compound nucleus can occur within an isolated quantum many-body system. Here, we approach modelling fusion with a time-dependent coupled channels model that does not require these conditions. Instead, incoming flux is trapped by allowing the wavefunction to couple to a large number of channels once inside the barrier. Results suggest that with sufficiently many channels included in the system, the transmission of the wavefunction through the potential barrier could be accurately reproduced without artificial flux-trapping conditions.

1 Introduction

When nuclei collide, some of the energy associated with their relative motion may be transferred to internal degrees of freedom, associated with the motion of constituent nucleons. This dissipation of energy into internal states plays an increasingly important role as reaction outcomes become more complex, from inelastic scattering to fusion. During fusion, the kinetic energy associated with relative motion must be entirely dissipated in order to form a compact, equilibrated compound nucleus.

The subsequent evolution of the compound nucleus is encapsulated in Bohr's independence hypothesis [1], which states that the decay of the compound nucleus is independent of its formation. This phenomenon emerges from the expectation that the compound nucleus is long-lived in comparison to the transit time of a nucleon across the nucleus. It implies that fusing systems lose information about the entrance channel. Bohr's hypothesis has been verified experimentally (see, for example, Refs [2, 3]) by comparing cross-bombardment reactions that produce the same compound nucleus with the same excitation energy and angular momentum.

Nuclear collisions are fast (~10^{-21} s [4]), and consequently well-isolated from interactions with their external environment. Time evolution in an isolated quantum system is unitary and hence reversible. However, the loss of information about the entrance channel that occurs during fusion makes the entrance channel irrecoverable and implies that fusion is irreversible. This makes fusion a good example of apparently irreversible dynamics occurring in an isolated, many-body quantum system. Understanding how this can arise in isolated quantum systems is currently an open question in quantum mechanics [5].

The coupled channels model is widely used to describe fusion [6]. The colliding nuclei are described by a linear superposition of channels that are allowed to couple together. Solutions of this system under the time-independent Schrödinger equation are found numerically. Typically, to model fusion a complex absorbing potential or an incoming wave boundary condition (IWBC) is applied inside the barrier region [6]. This removes the incoming flux that penetrates the fusion barrier, allowing the barrier transmission and fusion cross section to be calculated from the reduction in amplitude of the outgoing flux. However, it enforces irreversibility while obscuring any details about the energy dissipation involved.

Over the past two decades, several limitations of coupled channels models have become apparent. Coupled channels calculations are unable to simultaneously reproduce measurements for different reaction outcomes, such as elastic scattering and fusion, when using the same potential parameters [7, 8]. A similar problem is encountered when attempting to describe fusion at energies both above and below the barrier [9, 10]. These observations highlight the fact that coupled channels calculations require parameters to be tuned to match the specific problem at hand, rather than achieving a unified model that describes all reaction outcomes. It is widely agreed that a contributing factor to these limitations is an incomplete description of energy dissipation [10, 11].

Recent research has revealed that energy dissipation begins early in the reaction, even before capture [12]. The flux-trapping conditions of current models, applied inside the barrier, do not allow us to investigate dissipation that

*e-mail: maggie.webber@anu.edu.au

begins outside the barrier. This further motivates the development of an explicit description of energy dissipation.

In this article we present the first steps towards developing a dynamical coupled channels model for fusion without requiring an absorbing potential or IWBC. We present results suggesting that fusion may be described by allowing the system to couple to a sufficiently large number of channels inside the barrier, which act as a reservoir for energy dissipation. Importantly, this model provides an explicit description of dissipation among the many channels in the system.

2 Methods

To find solutions of the coupled channels equations in a time-dependent framework, we apply a time-dependent wavepacket method to solve the time-dependent coupled channels (TDCC) problem (Fig. 1). The initial wavepacket is localised far from the potential barrier where the potential is small, with some initial kinetic energy, E_0. As the system evolves, part of the wavepacket may tunnel through (or pass over) the barrier while the rest is reflected. Flux that remains inside the barrier for a long period of time can be identified with fusion. Using a time-dependent method thus allows us to identify fusion by taking advantage of the long timescale of fusion relative to other reaction outcomes.

To perform the time propagation we use the Chebyshev polynomial method [13], in which the time evolution operator is approximated as a polynomial expansion in the Hamiltonian, $\hat{H}$, of the system,

$$\exp\left(-\frac{i\hat{H}t}{\hbar}\right) = \sum_n a_n T_n(\hat{H}). \tag{1}$$

Here, T_n is the Chebyshev polynomial of degree n and a_n are expansion coefficients. This method is advantageous because the error in the numerical propagation associated with approximating the time evolution operator can be reduced to the limit of machine precision [13]. Then, the largest contribution towards numerical error is the application of the Hamiltonian, $\hat{H}$, itself.

In previous applications of the Chebyshev method to nuclear contexts (for example, Refs [14, 15]), the application of the kinetic energy component of $\hat{H}$ was calculated using a Fourier method. Fourier methods naturally enforce periodic boundary conditions, meaning that flux will continue past the $r = 0$ boundary and reappear at the other end of the spatial grid. With an absorbing potential inside the barrier this is not an issue, as incoming flux is captured before it can reach the boundary. Here, we use an 8th-order finite difference [16] to calculate the application of the momentum operator. This allows us to enforce a hard boundary at $r = 0$. The accuracy of the 8th-order finite difference is $O(\Delta x^8)$, limited by the spacing Δx between adjacent points of the spatial grid.

The method was verified by calculating the transmission through a Gaussian barrier for simple, two-channel coupled systems, reproducing results solved with time-independent methods in Ref. [17]. We then examined

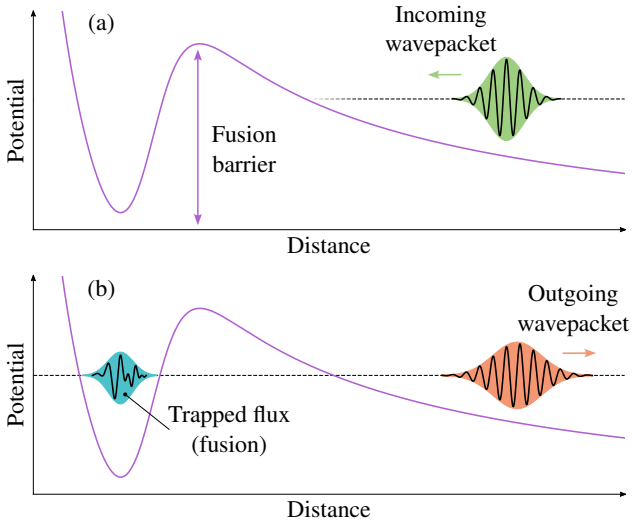

Figure 1. Diagram of the time-dependent coupled channels approach. (a) The initial wavepacket (green) is propagated forward in time under the internuclear potential (purple line). (b) At a later time $t = t_f$, most of the wavepacket (orange) has reflected from the potential barrier while a small part (blue) has tunnelled through.

^{16}O+^{208}Pb as it is well measured, and hence offers the opportunity to compare our model to experimental measurements and other theoretical models in the future. For the calculations presented in this paper, we used the internuclear potential from Ref. [10], consisting of an attractive Woods-Saxon potential with depth 100 MeV, radius 9.94 fm, and diffuseness 0.66 fm, and a sphere-Coulomb potential with radius 10.13 fm. The resulting potential barrier has a maximum of $V_B = 74.5$ MeV at radius $R_B = 11.95$ fm. For simplicity, the calculations presented here are performed with zero angular momentum.

A consequence of using time-dependent wavepacket methods is that a spatially localised wavepacket contains a range of different energy components, which currently we cannot resolve. We thus choose a spatially wide Gaussian initial wavepacket, with standard deviation $\sigma_0 = 150$ fm, so that the corresponding spread in energy is narrow ($\sigma_E \sim 0.13$ MeV). It was initialised at $r_0 = 2100$ fm, where the Coulomb tail of the potential varies by less than 0.15 MeV over the $2\sigma_0$ extent of the wavepacket. The entire spatial grid spanned 0–3500 fm, with spacing $\Delta r = 0.1$ fm between adjacent points.

Before considering the transmission of the wavepacket through the potential barrier in a coupled system, we performed calculations with an absorbing boundary at $r = 0$, performing the same function as an absorbing potential or IWBC. We verified that the resulting transmission of the wavepacket matches that found by numerically solving the time-independent Schrödinger equation with an absorbing potential inside the barrier. That is, with the inclusion of a flux-trapping condition, our time-dependent method coincides with time-independent solutions, as expected.

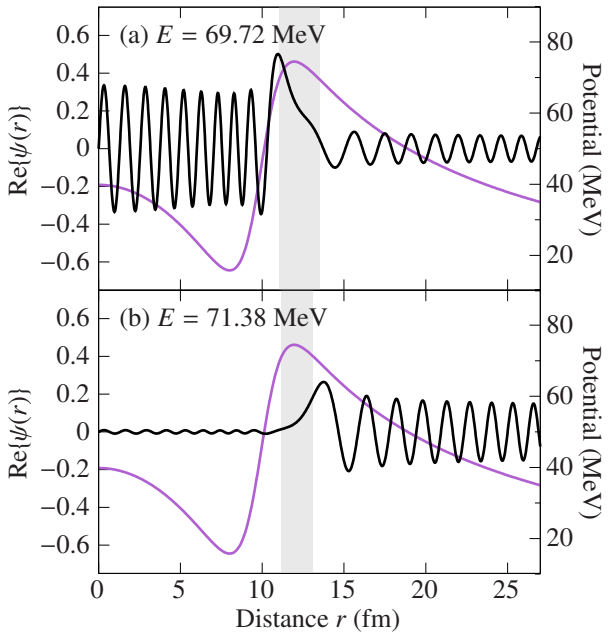

Figure 2. Real part of the wavefunction (black) at example (a) resonant and (b) non-resonant energies, found by numerically solving the time-independent Schrödinger equation. The right vertical axis shows the internuclear potential $V(r)$ (purple). The potential parameters are from Ref. [10], for ^{16}O+^{208}Pb (see text). The grey shaded area indicates the region where the wavefunction is classically forbidden, $E < V(r)$.

3 Resonances

Without an absorbing potential or IWBC inside the barrier, we need to consider the effect of resonances on the time-evolution of the system. Resonances occur at specific energies where the interior of the potential acts as a resonant cavity. For example, the potential used here for ^{16}O+^{208}Pb exhibits a resonance at E = 69.72 MeV. Near this energy, the transmission of the wavefunction through the potential barrier is enhanced, seen by the large amplitude of the static solution inside the barrier region, shown in Fig. 2a. In contrast, at non-resonant energies (Fig. 2b), the amplitude of the wavefunction is diminished inside the barrier.

Resonances are sensitive to the form of the potential. Allowing states to couple together modifies the potential, resulting in barrier splitting and barrier distributions [17]. Rather than interacting with a single potential, the coupled system can be considered to be interacting with a superposition of different potentials. Accordingly, the splitting of the potential causes the resonances to split and shift in energy. The more channels available, the more the resonances will fragment, changing the fraction of the flux that penetrates the barrier. With sufficiently many couplings, we might expect to approximate the actual behaviour of the compound nucleus and its formation.

4 Modelling fusion without an absorbing potential or IWBC

Coupled channels calculations typically include only a few channels, focussing on the dominant states involved in the reaction. In reality, a large number of internal states are involved in fusion, as energy is dissipated among the many internal states of the compound nucleus.

We propose that for the purpose of modelling fusion, it may be possible to approximate the many internal states of the compound nucleus by allowing the system to couple to a large number of channels once inside the barrier, producing a broad, densely populated spectrum of resonances accessible only via coupling at short distances inside the barrier. This enables the wavefunction to be trapped without needing an absorbing potential or IWBC.

As more channels are included in the system, we expect that the exact details of the individual channels and couplings will become less important. Coupling to one reservoir of many coupled channels should be much the same as coupling to another, provided that they share similar overall properties (i.e., the excitation energies of the states and the couplings between them are on the same order of magnitude).

To test this, we performed calculations at an off-resonance energy, E = 71.5 MeV, with an increasing number of channels included in the system. Each pair of channels is coupled together by a Woods-Saxon coupling potential with a randomly chosen strength between 0–1 MeV. The radius R_C = 3.98 fm and diffuseness a_C = 0.33 were chosen so that the coupling potential was entirely localised inside the barrier radius. The excitation energies E_x of the channels are evenly spaced between 0–3 MeV, with the entrance channel having E_x = 0 MeV. For each system of N channels, we performed calculations for 20 different sets of random couplings. To ensure that observed differences are due to the number of channels rather than the individual couplings, the channels and couplings of smaller systems were chosen as subsets of the largest (N = 512) systems.

As a proxy for the transmission of the wavefunction through the barrier, we calculate the total norm of the wavefunction inside the barrier radius. Example calculations, as a function of time, are shown in Fig. 3 for an increasing number of channels. The dashed line in Fig. 3a shows the result for a single channel (no coupling). For this single-channel calculation, the amount of flux inside the barrier region increases over time as the incoming wavefunction arrives, and then decreases while the bulk of the wavefunction reflects from the barrier and the flux immediately exits the barrier region. The amount of flux inside the barrier at any one time is always lower than the total expected transmission (grey horizontal line), as the spatial width of the wavepacket is large relative to the barrier radius. By the time the later parts of the wavepacket reach the barrier, the earlier parts have already left. This single-channel result illustrates that off-resonance energies transmitted through the barrier do not remain trapped.

Once couplings are introduced, even with only N = 8 channels (Fig. 3a), the amount of trapped flux at any one

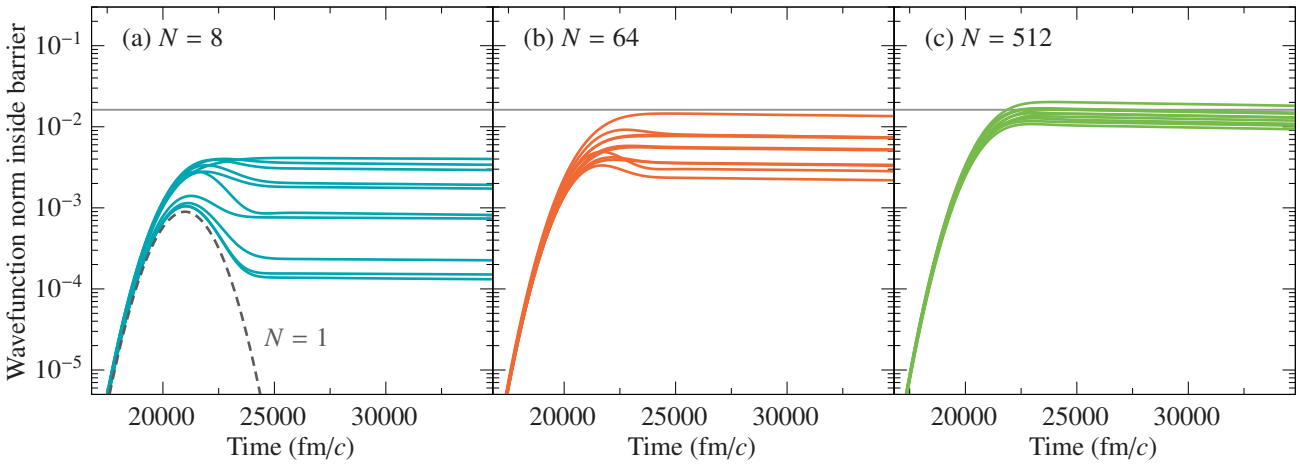

Figure 3. Norm of the wavefunction inside the barrier region ($r < R_B = 11.95$ fm) over time for calculations at $E = 71.5$ MeV with (a) $N = 8$, (b) $N = 64$, and (c) $N = 512$ channels included in the model. The channels are allowed to couple together inside the barrier region (see text). Here, 10 different coupling schemes are shown, each with different, randomly selected coupling strengths between each pair of channels. The horizontal line shows the expected transmission of the wavepacket through the potential barrier, calculated by numerically solving the time-independent Schrödinger equation for the range of energies contained in the initial wavepacket. The dashed grey line in (a) shows the wavefunction norm over time for a single-channel system, with no coupling.

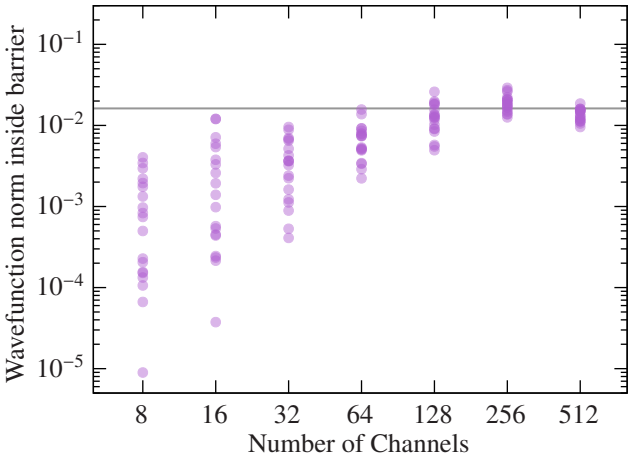

Figure 4. Flux remaining inside the barrier region at time $t_f = 32500$ fm/c. For each number of channels, there are 20 different coupling schemes with randomly chosen coupling strengths between each pair of channels (see text). The grey horizontal line shows the expected transmission through the potential barrier.

time is substantially increased. However, the amount of flux that remains trapped inside the barrier varies by some orders of magnitude, depending on the couplings between channels. As the number of channels increases, to $N = 64$ (Fig. 3b) and $N = 512$ (Fig. 3c), the wavefunction norm inside the barrier region becomes more consistent across the different sets of random couplings. Furthermore, the amount of flux trapped inside the barrier region at long times, after the rest of the wavefunction has reflected, approaches the expected transmission (grey horizontal line).

A more detailed picture is presented in Fig. 4, showing the norm of the wavefunction inside the barrier at time $t_f = 32500$ fm/c. Each point shows the result from a different set of random couplings, of which there are 20 for each N. As the number of channels increases, the amount of trapped flux becomes less dependent on individual couplings and approaches the transmission expected from a single channel calculation with an absorbing potential.

A surprising feature of the results presented Fig. 4 is that for some coupling schemes, the amount of flux inside the barrier region can exceed the expected transmission through the barrier. This may be a result of the coupling potential extending weakly into the barrier region, slightly enhancing the transmission. To prevent this from occurring, we could restrict the coupling potential to shorter distances and increase how steeply it falls off before the barrier. It should be noted that a sharp cutoff of the coupling potential is not a good option as it will induce reflections. This may also explain some of the variation in the norm inside the barrier amongst the different random coupling schemes.

5 Conclusion

We investigated a new approach to describe fusion using a time-dependent coupled channels model. The wavefunction is allowed to couple to a large reservoir of channels inside the fusion barrier. These produce a densely populated spectrum of resonances, trapping the wavefunction inside the barrier without an absorbing potential.

Our results suggest that with enough channels, outcomes become independent of the nature of the couplings between the channels. With an increasing number of channels, the transmission of the wavefunction through the potential barrier approaches that expected from time-independent calculations. Further work is required to understand exactly how many channels and couplings are required for the solution to converge to arbitrary precision, and to quantify the effect of the overall strength of

the couplings. To benchmark our new method, future work will also require comparison to established time-independent coupled channels codes, such as CCFULL [18] or FRESCO [19].

Our method explicitly (albeit phenomenologically) describes the dissipation of incoming flux a mong many states. This provides insight into the mechanisms that drive energy dissipation in nuclear reactions, and a framework to investigate the onset of dissipation in superheavy element formation reactions. Furthermore, it may shed light on the apparent irreversibility inherent to fusion, as described by Bohr's independence hypothesis, and the emergence of irreversible phenomena in a fully coherent quantum system.

Acknowledgements

The authors acknowledge support from the Australian Research Council through Discovery Grants DP250101791 and DP230101028. M. M. W. acknowledges support from an Australian Government Research Training Program scholarship.

References

[1] N. Bohr, Neutron Capture and Nuclear Constitution, Nature **137**, 344 (1936). 10.1038/137344a0

[2] S.N. Ghoshal, An Experimental Verification of the Theory of Compound Nucleus, Physical Review **80**, 939 (1950). 10.1103/PhysRev.80.939

[3] J. Silano, A. Tonchev, R. Henderson, N. Schunck, W. Tornow, C. Howell, F.N.U. Krishichayan, S. Finch, Validating the Bohr hypothesis: Comparing fission-product yields from photon-induced fission of ^{240}Pu and neutron-induced fission of Pu, EPJ Web of Conferences **239**, 03004 (2020). 10.1051/epjconf/202023903004

[4] C. Simenel, K. Godbey, A. Umar, Timescales of Quantum Equilibration, Dissipation and Fluctuation in Nuclear Collisions, Physical Review Letters **124**, 212504 (2020). 10.1103/PhysRevLett.124.212504

[5] J. Eisert, M. Friesdorf, C. Gogolin, Quantum many-body systems out of equilibrium, Nature Physics **11**, 124 (2015). 10.1038/nphys3215

[6] K. Hagino, K. Ogata, A.M. Moro, Coupled-channels calculations for nuclear reactions: From exotic nuclei to superheavy elements, Progress in Particle and Nuclear Physics **125**, 103951 (2022). 10.1016/j.ppnp.2022.103951

[7] J.O. Newton, R.D. Butt, M. Dasgupta, D.J. Hinde, I.I. Gontchar, C.R. Morton, K. Hagino, Systematic failure of the Woods-Saxon nuclear potential to describe both fusion and elastic scattering: Possible need for a new dynamical approach to fusion, Physical Review C **70**, 024605 (2004). 10.1103/PhysRevC.70.024605

[8] A. Mukherjee, D.J. Hinde, M. Dasgupta, K. Hagino, J.O. Newton, R.D. Butt, Failure of the Woods-Saxon nuclear potential to simultaneously reproduce precise fusion and elastic scattering measurements, Physical Review C **75**, 044608 (2007). 10.1103/PhysRevC.75.044608

[9] C.R. Morton, A.C. Berriman, M. Dasgupta, D.J. Hinde, J.O. Newton, K. Hagino, I.J. Thompson, Coupled-channels analysis of the ^{16}O+^{208}Pb fusion barrier distribution, Physical Review C **60**, 044608 (1999). 10.1103/PhysRevC.60.044608

[10] M. Dasgupta, D.J. Hinde, A. Diaz-Torres, B. Bouriquet, C.I. Low, G.J. Milburn, J.O. Newton, Beyond the Coherent Coupled Channels Description of Nuclear Fusion, Physical Review Letters **99**, 192701 (2007). 10.1103/PhysRevLett.99.192701

[11] K. Hagino, N. Takigawa, Subbarrier fusion reactions and many-particle quantum tunneling, Progress of Theoretical Physics **128**, 1061 (2012). 10.1143/PTP.128.1061

[12] K.J. Cook, D.C. Rafferty, D.J. Hinde, E.C. Simpson, M. Dasgupta, L. Corradi, M. Evers, E. Fioretto, D. Jeung, N. Lobanov et al., Colliding heavy nuclei take multiple identities on the path to fusion, Nature Communications **14**, 7988 (2023). 10.1038/s41467-023-43817-8

[13] H. Tal-Ezer, R. Kosloff, An accurate and efficient scheme for propagating the time dependent Schrödinger equation, The Journal of Chemical Physics **81**, 3967 (1984). 10.1063/1.448136

[14] M. Boselli, A. Diaz-Torres, Quantifying low-energy fusion dynamics of weakly bound nuclei from a time-dependent quantum perspective, Physical Review C **92**, 044610 (2015). 10.1103/PhysRevC.92.044610

[15] T. Vockerodt, A. Diaz-Torres, Describing heavy-ion fusion with quantum coupled-channels wave-packet dynamics, Physical Review C **100**, 034606 (2019). 10.1103/PhysRevC.100.034606

[16] B. Fornberg, Generation of Finite Difference Formulas on Arbitrarily Spaced Grids, Mathematics of Computation **51**, 699 (1988). 10.1090/s0025-5718-1988-0935077-0

[17] C.H. Dasso, S. Landowne, A. Winther, Channel-coupling effects in heavy-ion fusion reactions, Nuclear Physics A **405**, 381 (1983). 10.1016/0375-9474(83)90578-X

[18] K. Hagino, N. Rowley, A.T. Kruppa, A program for coupled-channel calculations with all order couplings for heavy-ion fusion reactions, Computer Physics Communications **123**, 143 (1999). 10.1016/S0010-4655(99)00243-X

[19] I.J. Thompson, Coupled reaction channels calculations in nuclear physics, Computer Physics Reports **7**, 167 (1988). 10.1016/0167-7977(88)90005-6